Journal of
Applied Remote Sensing

County-level rice area estimation in southern China using remote sensing data

Qiangzi Li
Huanxue Zhang
Xin Du
Ning Wen
Qingshan Tao

County-level rice area estimation in southern China using remote sensing data

Qiangzi Li,[a,*] Huanxue Zhang,[a] Xin Du,[a] Ning Wen,[b,c] and Qingshan Tao[b,c]

[a]Chinese Academy of Sciences, Institute of Remote Sensing and Digital Earth, State Key Laboratory of Remote Sensing Science, and National Engineering Research Center for Geoinformatics, Beijing 100101, China

[b]Hunan Research Academy of Geological Sciences, Changsha 410007, China

[c]Hunan Planning Institute of Land and Resources, Changsha 410007, China

Abstract. Rice acreage estimation is a key aspect of assessing rice production. A method of estimating rice acreage at the county level is explored, using data from the HJ-1A/B Chinese Environmental Satellite for Hunan Province, which has complex rice cropping patterns. The method combines supervised and unsupervised classification using a mixed-pixel decomposition model. The rice acreage estimation results were validated by interpretation of RapidEye images for early-season rice and ground survey data for medium-season and late-season rice. The results showed a good correlation between the estimates derived from RapidEye and from HJ CCD data for pure rice pixels ($R^2 = 0.99$, 0.99, and 0.97 for early-, medium-, and late-season rice). The discrepancy was <10% at the plot level (6.5×6.5 km) for early-season rice, while it was 12.20 and 12.36% at the plot level (1×1 km) for medium-season and late-season rice. These results suggested that the method proposed in this study is capable of rice acreage estimation at the county level. The method can also be used in mountainous regions and areas of fragmented planting. [DOI: 10.1117/1.JRS.8.083657]

Keywords: rice; acreage; remote sensing; county; grain subsidy.

Paper 13519 received Dec. 9, 2013; revised manuscript received Feb. 18, 2014; accepted for publication Feb. 25, 2014; published online Mar. 26, 2014.

1 Introduction

Paddy rice is the second most widely planted grain crop in the world, accounting for >11% of global cultivated area.[1] Almost half the world's population use rice as a main staple food, especially in Asia. In China, rice is planted from the tropical zones in the south to the temperate zones in the northeast and provides ~40% of total grain production. With the development of the economy, the rate of return on planting grain crops has decreased. Many farmers have shifted from a double-cropping to a single-cropping scheme. To provide incentives to farmers for grain cultivation, the Chinese central government has introduced subsidies. One crop per season is still the practice in Hunan, Jiangxi, and Zhejiang provinces.

Statistical data from local governments have always been used to calculate the subsidies. However, large discrepancies are often observed between different datasets from different governmental departments or agencies. Therefore, reliable methods need to be developed to extract accurate and reliable rice crop acreage estimates to support governmental agricultural policy.

Remote sensing has been widely used for regional crop acreage estimation in the last 30 years.[2–5] Single- or multitemporal high-resolution images have been used to identify crop types using various image classifiers.[6–8] Normalized difference vegetation index (NDVI) time series datasets have also been used to discriminate among various crops by extracting crop phenological information.[9–12] To promote accurate crop acreage estimation, subpixel classification using linear unmixing or neural networks has also been developed to estimate the fractions of various crops within every pixel.[13–15]

*Address all correspondence to: Qiangzi Li, E-mail: liqz@radi.ac.cn

0091-3286/2014/$25.00

Moreover, the multitemporal synthetic aperture radar (SAR) backscatter coefficient has been used to reflect changes in rice crop height or roughness in fields with growing rice crops.[16] Multipolarized SAR data have also been used to construct parameters, such as the ratio between cross-polarization (HV) and co-polarization (VV), to distinguish rice crops from other vegetation.[17] To support grain subsidy policies in southern China, a more reliable and practical method is needed, with an acreage monitoring accuracy >85% in each county where data are required by the government. The challenge lies in the following two aspects: (1) Crops of different seasons are often interplanted within very small fields, 768 m^2 on average.[18] Early-season rice, early-season single rice, and medium-season rice are sometimes planted side by side at only two-week intervals. Hence, the similarity of spectral signals among crops from different seasons increases the difficulty of pixel-based classification. (2) Rainy or cloudy weather conditions often occur during the rice growing season in southern China. Optical images, therefore, cannot provide full coverage of planted areas during the growing season.

In this study, a method has been developed to identify rice plantings of different seasons and to estimate their acreage using wide-swath high-spatial-resolution multispectral images. The objectives include the following: (1) investigating the feasibility of identifying various rice plantings of different seasons using remotely sensed images and (2) developing a practical method of estimating rice acreage at the county level in southern China.

2 Study Area

In this study, Hunan Province, which contributes 13% of the total rice production of China, was selected as the study area. Hunan is located to the south of the Yangtze River and Dongting Lake (24.63° to 30.13°N, 108.78° to 114.25°E; Fig. 1) with 122 counties. The province is surrounded by mountains except to the north. The total land area is ~211,829 km^2, of which 37,890 km^2 are arable land. Paddy rice accounts for >90% of crops (paddy rice, potatoes, corn, and wheat, etc.) in the Xiangjiang River Basin and along the fringe of Dongting Lake, while dry-land crops are distributed mainly in the western and southern mountainous areas.[19]

The climate in the region is a typical subtropical humid monsoon climate, which is favorable to complex multiseason rice cropping systems. The major rice cropping systems are double-season rice in most of the Dongting Lake and Xiangjiang River Basins, and single-season rice in most of the western area and some areas in the eastern part of the province. Early-season rice is sown in late April and harvested in early July. Late-season rice is sown in early July and

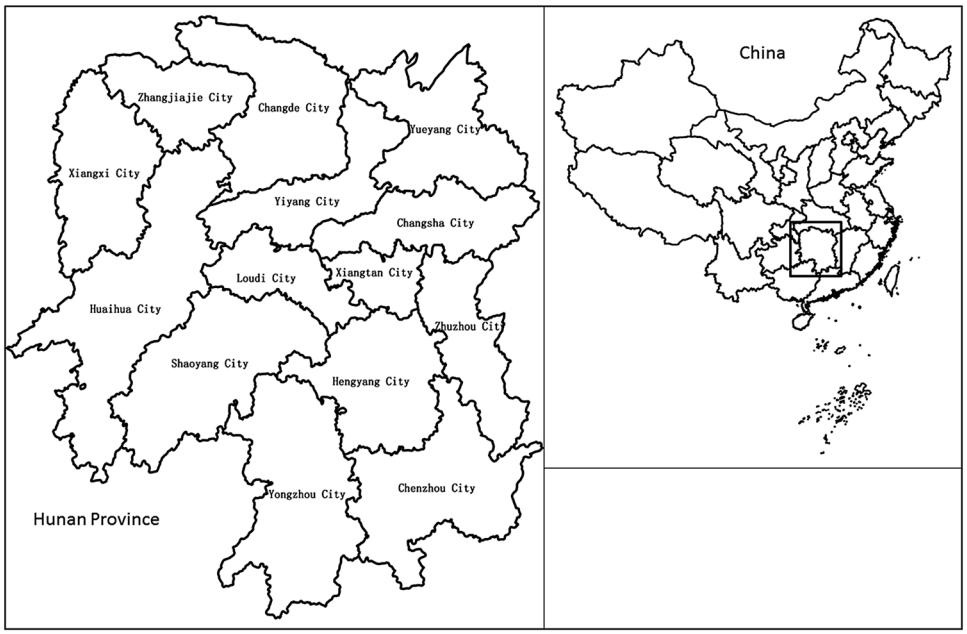

Fig. 1 Location of the study area.

harvested in late October. Traditionally, the medium-season rice is transplanted in May and harvested early in September (Table 1). Recently, single-season early rice and single-season late rice have become a more common cropping practice. Single-season early rice is usually planted three weeks earlier than medium-season rice and single-season late rice usually three weeks earlier than late-season rice.

3 Data and Preprocessing

3.1 *Remote Sensing Data*

In this study, HJ-1 CCD images were used as the main source of remote sensing data. The two multispectral CCD sensors uploaded on the HJ-1 A and B satellites can provide scans with a 360-km swath at 30-m spatial resolution with a revisit period of 4 or 5 days. The CCD sensors contain four spectral wavebands ranging from 430 to 900 nm.[20] Twenty-seven HJ-1 CCD registrations were acquired during the growing season from May to October 2012 (Fig. 2).

The preprocessing of HJ-1 CCD images included radiance calibration, atmospheric correction, and geocorrection. Radiance calibration was performed using the formula $\rho = (\mathrm{DN}/\mathrm{C0} + \mathrm{M0}) \times \cos\,\theta$, where ρ is the surface spectral reflectance, θ is the solar altitude angle, C0 is the absolute calibration constant gain, and M0 is the offset. Atmospheric correction was carried out using the second simulation of the satellite signal in the solar spectrum model.[21]

Geometrical correction was conducted using a quadratic polynomial method based on high-spatial-resolution aerial photographs, and the error was controlled within 0.5 pixels.

Two RapidEye multispectral images with 5.8-m spatial resolution were acquired for validation purposes on June 19 and 24, 2012 (Fig. 2).

3.2 *Arable Land Dataset*

An arable land dataset was extracted from the second National Resource Investigation database at 1 : 10,000 scale (Fig. 3). The dataset was derived from interpretation of airborne or very-high-spatial-resolution (VHR) satellite images, including SPOT merged images using XS and panchromatic data and Quickbird images. The dataset was used to mask nonarable regions within the HJ-1 CCD images. Gross and net cropland area figures were also included in the dataset.

Together with the arable land dataset, a nonarable coefficient (NAC) database was also collected to calculate net crop acreage. The data values were calculated from ground surveys and measurements at the patch level. For each arable land patch, NAC considered all nonarable objects smaller than the mapping scale.

3.3 *Other Datasets*

Administrative, provincial, district, and county boundary datasets at 1 : 100,000 scale were collected (Fig. 1). A road dataset was also collected, including expressways, national highways, provincial highways, and local roads.

Table 1 Rice crop calendar in Hunan Province.

Rice crop	April			May			June			July			August			September			October		
early-season rice																					
single-season early rice																					
medium-season rice																					
single-season late rice																					
late-season rice																					

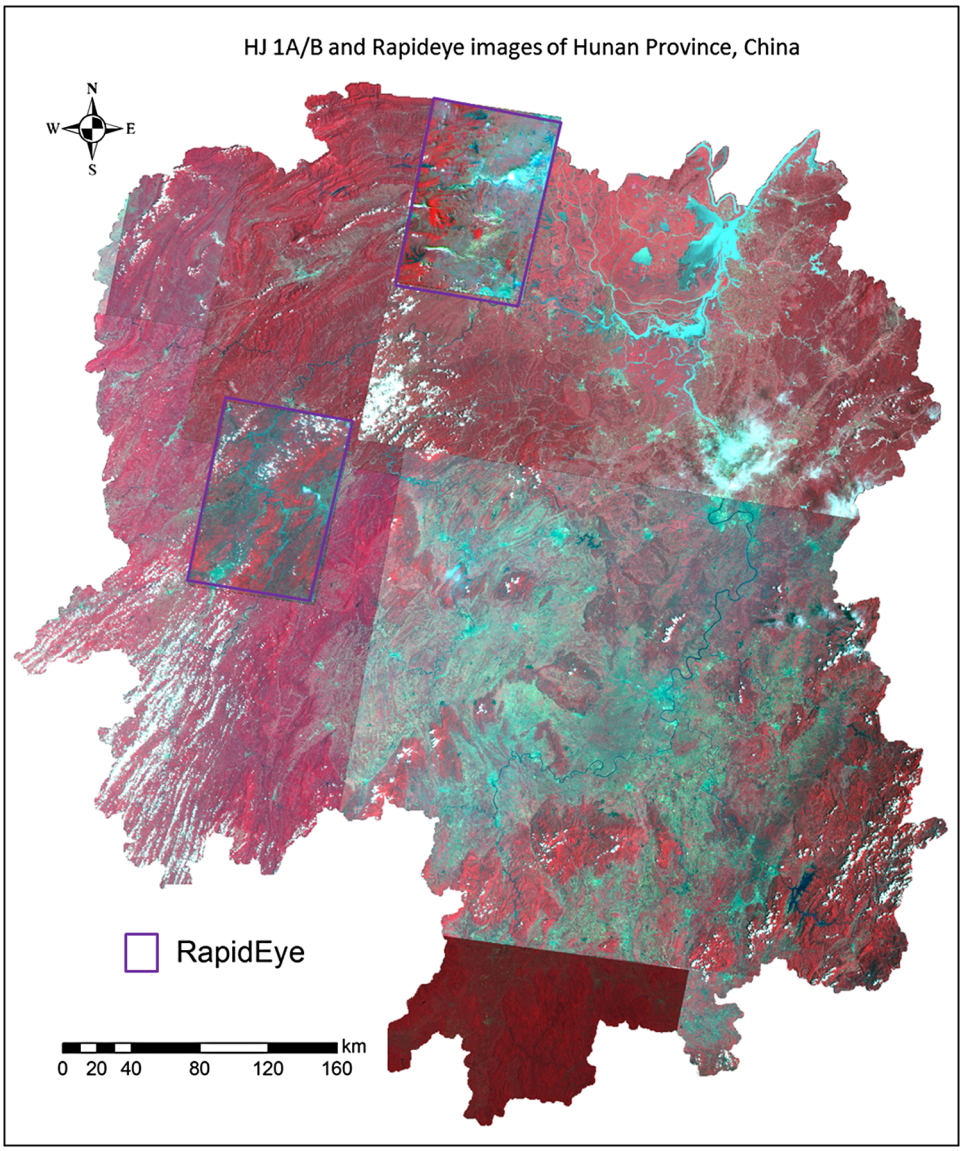

Fig. 2 HJ CCD and RapidEye images used in Hunan Province.

4 Methods

Normally, rice is grown on irrigated or rain-fed paddy fields in southern China. Hence, rice acreage estimation involved only paddy field investigations. Improving rice identification accuracy by screening out nonpaddy field areas within the images using the arable land dataset proved to be an effective approach. Medium-season rice, early-season rice, and late-season rice are always planted side by side, and it is very difficult to discriminate different seasons of rice within remotely sensed images through image classification. According to rice phenology, there is a monitoring window of 1 month for early-season rice and 2 months for late-season rice. For medium-season rice identification, early-season rice and late-season rice identification results can offer assistance for determination of single- or double-cropped rice, as well as for image classification. If a pixel is not identified as early rice or as late rice, but spectral analysis identifies crops within it, this means that the pixel is probably a medium-rice parcel.

Maximum likelihood classification (MLC), artificial neural networks (ANNs), and support vector machine (SVM) classifiers are often involved in crop identification from remotely sensed images. The SVM classifier appears to be more accurate than MLC and ANN classifiers when dealing with temporally infrequent images.[22] Hence, the SVM classifier was used by preference

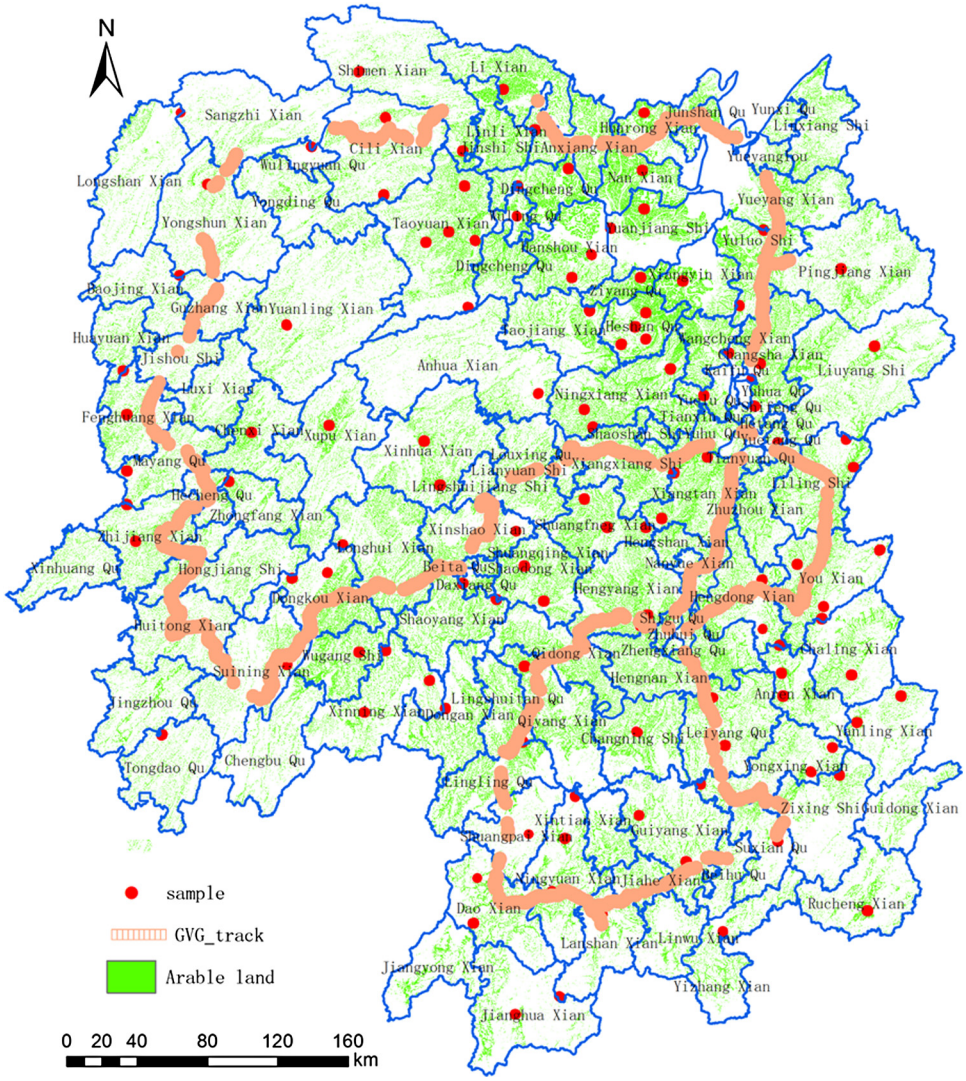

Fig. 3 Distribution of arable land, sampling blocks, and transect routes in Hunan Province.

in this study. *In situ* investigations or field surveys were conducted to collect ground training data for image classification.

Due to the household-based land allocation policy of China, rice parcels are very small. Hence, rice parcels with different planting seasons are mixed together, and discriminating them within 30-m resolution images is infeasible. Therefore, a subpixel classification method was used to obtain accurate rice acreage estimates. Rice acreage can be normally estimated by statistical pixels of different rice crops. However, small or linear nonarable objects, such as roads and small ponds, cannot reflect in the spectrum of the pixels. Consequently, NAC, which is collected on the county level, must be used to verify the estimation results. In addition, the estimated acreage figures should also be calibrated using figures from a ground survey.

As described above, a special method for rice acreage estimation has been developed to derive the county-level acreage of different rice crops (Fig. 4).

4.1 *Ground Survey*

To collect *in situ* crop parcel information, 122 plots, 1 by 1 km^2 in area, were arranged through systematic sampling. First, a grid layer with 4 by 4-km^2 cells was generated using geographic information system (GIS) tools. There were ~2,000,000 blocks for the entire province, which were stratified into five strata according to the paddy field density (>80%, 50 to 80%, 30 to 50%,

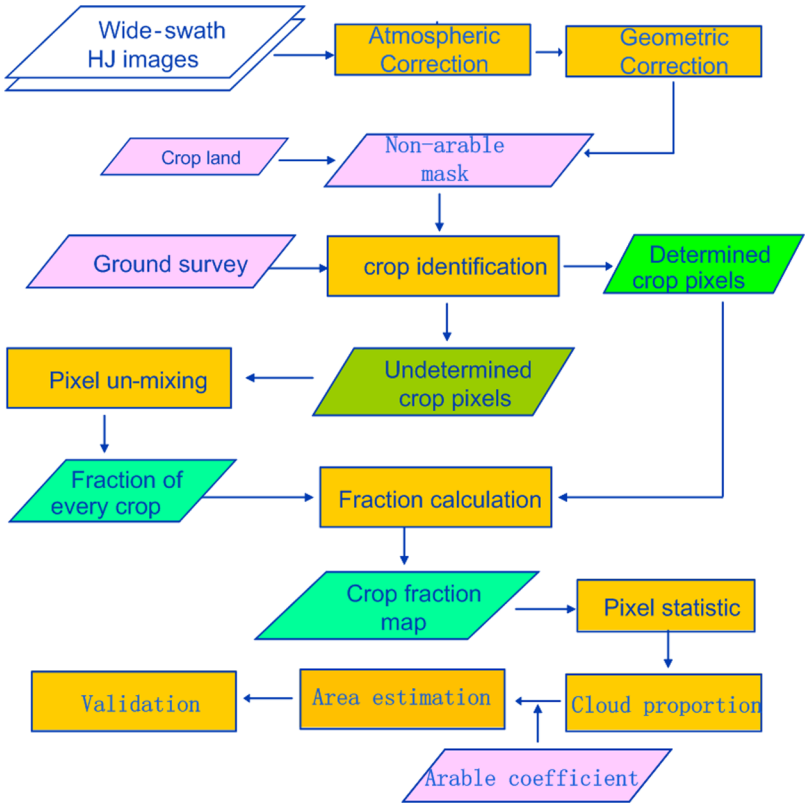

Fig. 4 Flow chart of county-level rice acreage estimation using remote sensing.

15 to 30%, <15%). Then a 2% sampling ratio was used to select sampling blocks proportionally distributed in the five clusters by their paddy field acreage (Fig. 3). For the ground survey, every sampling block was systematically split into 4×4 plots. Then the ground surveyors selected one plot to map crop parcels.

Before the survey, very-high-resolution images, such as aerial photos at 1 m, were used to digitize the boundaries of crop parcels in the office. Then, on-site teams carried out the survey and registered the parcels using mobile GIS tools. At the same time, transect sampling were also performed using global position system-video-GIS (GVG) agro-sampling instruments.[4] In total, 2500 km of routes were defined, and geotagged photos were collected along the sampling routes to compensate for the deficiencies of the ground survey in certain areas (Fig. 3).

4.2 *Spectral Training and Image Classification*

The ground truth dataset included 3411 parcels, of which 260 were early-season rice, 805 medium-season rice, 637 late-season rice, and 1709 nonvegetated areas. Among these, five parcels of early-season rice, 102 parcels of medium-season rice, 337 parcels of late-season rice, and 932 of nonvegetated areas were used for training and the rest of the dataset for validation. For rice crop identification, the SVM was adapted to perform image classification.

HJ CCD images during the optimal observation phase were acquired to identify different season rice crops. For early-season rice identification, images in May were the best choice, followed by images in the first 10 days of June. For late-season rice identification, images after the harvest of medium-season rice were preferred. For medium-season rice identification, multitemporal images were used (Fig. 5).

4.3 *Treatment of Mixed Pixels in HJ CCD Images*

Pixel-level rice crop classification can only identify pure rice crop pixels. Mixed pixels were classified as other crops. The rice area fraction index (RAFI) was used to depict the area

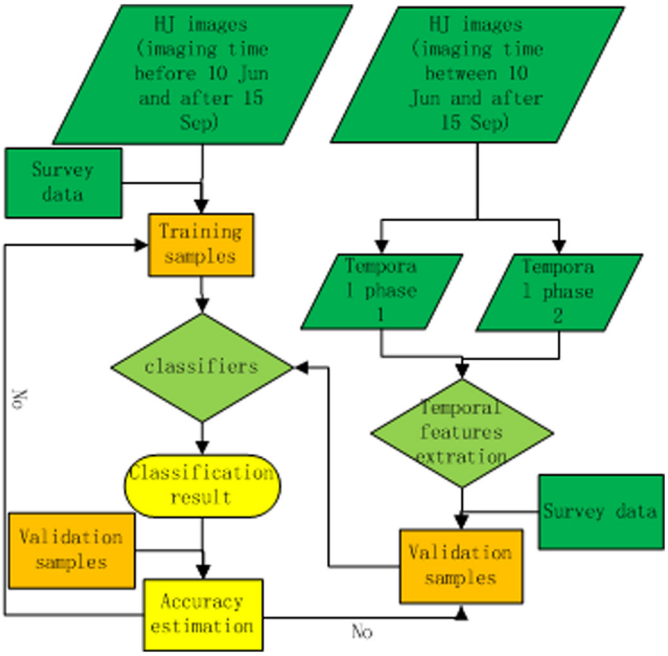

Fig. 5 Identification of early/late-season rice crops using single-temporal HJ CCD and medium-season rice using multitemporal HJ CCD data.

proportion within each pixel. When only early-season rice or late-season rice is growing in the paddy fields, RAFI is equivalent to *fcover*, which is widely used in vegetation ecosystem monitoring using remote sensing. Various *fcover* estimation methods have been developed; the most widely used method for extracting compositional information from remotely sensed images is linear mixture modeling. In this study, a method based on NDVI was used to calculate RAFI. The method is expressed in Eqs. (1) and (2).

$$\mathrm{VI} = \sum f_i \mathrm{VI}_i = f_\mathrm{r}\mathrm{VI}_\mathrm{r} + f_\mathrm{bs}\mathrm{VI}_\mathrm{bs}, \tag{1}$$

$$\sum f_i = f_\mathrm{r} + f_\mathrm{bs} = 1, \tag{2}$$

where VI represents the NDVI of a pixel composed of mixed vegetation and bare soil, VI_r represents the average NDVI value of a rice crop, VI_bs represents the average NDVI value of bare soil, f_r represents the area fraction of rice crop within the pixel, and f_bs represents the area fraction of bare soil within the pixel.

The NDVI can then be calculated as follows:

$$\mathrm{NDVI} = \frac{R_\mathrm{nir} - R_\mathrm{red}}{R_\mathrm{nir} + R_\mathrm{red}}, \tag{3}$$

where R_nir and R_red represent the reflectances of the near-infrared and red bands, respectively, which correspond to the fourth and third bands in HJ-1A/B images.

When carrying out RAFI estimation, mixed rice pixels should be identified first. In this study, unsupervised classification using the ISODATA algorithm was used first to identify pixels containing rice. Then, mixed rice pixels can be identified by screening the pure rice pixels.

4.4 *Rice Acreage Estimation*

Rice acreage estimation was performed in this study by integrating accumulated pixel-level RAFI and ground survey data. Pixel-level RAFIs were first used to calculate county-level

gross area figures for various rice crops, and then the nonarable land coefficient from the second National Resource Survey database was used to derive the net area figures. When an area was overlapped by multitemporal images for one type of rice growing season, the results with the highest classification accuracies were selected first.

Abnormal conditions, especially cloud coverage, must also be considered. Because of the prevalence of cloudy or foggy days in southern China, there may always be some areas that cannot be covered by cloud-free images even if wide-swath CCD data are used. In this study, a parameter r_c, defined as the ratio of cloudy area to the total area of the county, was introduced to resolve uncertainty due to cloudy conditions. Finally, the rice acreage was calculated using Eq. (4).

$$S = \frac{\sum_{p=i}^{n} A_p \times (1 - r)}{1 - r_c}, \tag{4}$$

where S is the regional crop planting acreage, A_p is the crop pixel acreage, r is the nonarable coefficient, and r_c is the cloud proportion.

4.5 *Validation and Accuracy Assessment*

4.5.1 *Accuracy assessment of rice crop identification*

Accuracy assessment was carried out using an independent validation dataset generated from field surveys. Accuracy evaluation included the overall classification accuracy and estimation of kappa statistics from the confusion matrix.[23] In this study, accuracy was evaluated as the percentage of pixels correctly classified.

$$\text{accuracy} = \frac{\sum_{k=1}^{q} n_{kk}}{n} \times 100\%, \tag{5}$$

where n is the number of validation pixels, q is the number of classes, and n_{kk} is the number of pixels correctly classified for each class.

The confusion matrix is used to provide information on the accuracy of the mapping result as applied to an independent set of observations. Information in the error matrix can be evaluated using simple descriptive statistics, such as overall accuracy, producer's accuracy, and user's accuracy, or by multivariate statistical analysis techniques. At the same time, the kappa coefficient was also calculated to assess comparative accuracy,[24,25] which compares the level of agreement against that which might be expected by chance.[26]

4.5.2 *Accuracy assessment of rice crop acreage estimation*

Rice crop acreage estimates from HJ CCD image classification were compared to *in situ* survey data at the plot level (1×1 km). Relative discrepancy was used to assess estimation accuracy using Eq. (6).

$$\text{RD} = \frac{A_1 - A_0}{A_0} \times 100\%, \tag{6}$$

where RD is the relative discrepancy, A_1 is the rice crop acreage from HJ CCD data, and A_0 is the rice crop acreage from *in situ* data.

For early-season rice area estimation in 2012, RapidEye image classification was used to replace *in situ* survey data and was considered as ground truth. With classification at 5.8-m spatial resolution, it is plausible that the two RapidEye images can produce a rice crop distribution and result in accurate rice crop acreage estimation. In this study, 12 plots 6.5×6.5 km in size within each RapidEye image were selected to evaluate the acreage figures (Fig. 6). Relative discrepancies were also calculated to assess the accuracy of early-season rice acreage estimation.

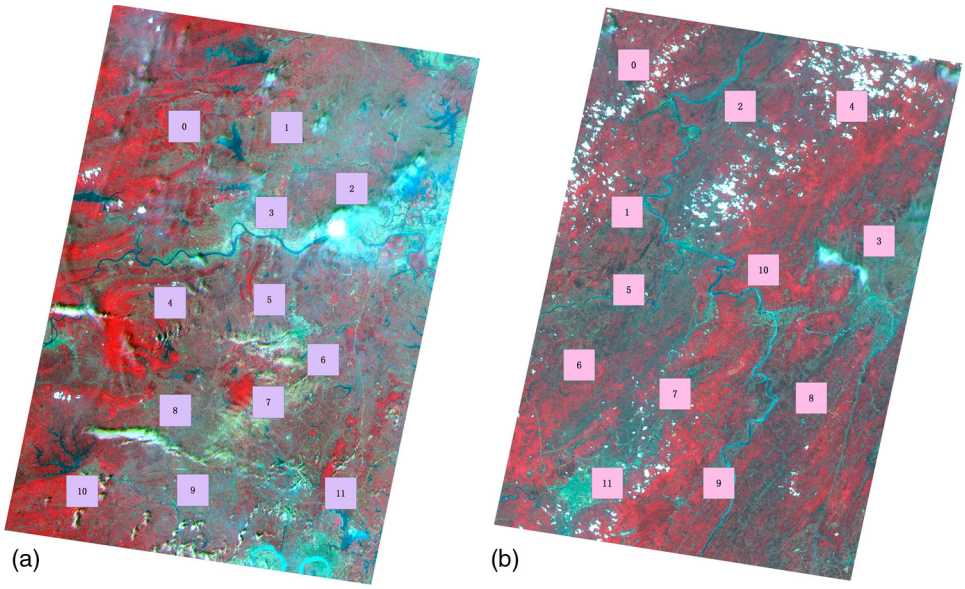

Fig. 6 Plot locations for early-season rice crop acreage validation in 2012: (a) Imaging date of June 19, 2012. (b) Imaging date of June 24, 2012.

5 Results

5.1 *Ground Survey and Results*

In 2012, field observations were carried out during mid-to-late August, which is in the growing season for the medium-season and late-season rice. Figure 7(b) shows an example *in situ* crop map within a plot, while Fig. 7(a) shows an HJ-1 CCD image of the same area.

Using transect sampling, 6465 geotagged field photos were collected with the help of transect sampling instruments, of which 313 were used for late-season rice crop identification and 279 for medium-season rice identification.

5.2 *Rice Crop Pixel Identification Results*

Through rice crop identification using HJ CCD data, pure rice crop pixels can be accurately identified. Table 2 gives the overall accuracies and kappa coefficients for rice crop identification. Accuracy assessment results showed very high crop identification accuracy. For early-season rice identification, the average kappa coefficient was ~0.956, with an overall classification

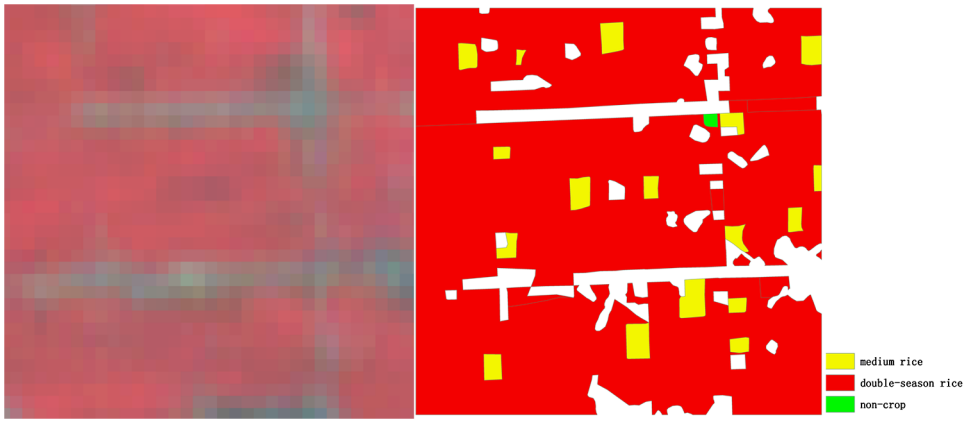

Fig. 7 Samples of crop map within plots: (a) Enlarged area of HJ-1 CCD image in 2012. (b) Example *in situ* crop map in a sampling plot.

Table 2 The distribution of classification errors and kappa coefficient with HJ CCD in 2012.

No. of HJ CCD images	Overall accuracy (%)	Kappa	Target rice crop
5-84-20120518	97.89	0.9618	Early-season rice
6-80-20120520	99.72	0.9958	Early-season rice
2-81-20120619	98.34	0.9744	Early-medium season rice
456-84-20120620	98.91	0.9855	Early-medium season rice
4-80-20120623	99.82	0.9975	Early-medium season rice
2-84-20120704	99.08	0.9867	Early-medium season rice
457-82-20120707	99.69	0.9959	Early-medium season rice
457-84-20120707	97.05	0.9557	Early-medium season rice
457-84-20120722	92.67	0.8934	Medium-season rice
5-80-20120730	99.94	0.9991	Medium-season rice
4-84-20120730	77.15	0.6819	Medium-season rice
5-85-20120801	95.39	0.9305	Medium-season rice
2-80-20120818	96.2	0.9347	Late-medium season rice
2-84-20120820	92.86	0.8938	Late-medium season rice
6-84-20120828	98.08	0.972	Late-medium season rice
4-80-20120829	95.5	0.9285	Late-medium season rice
4-88-20120829	89.21	0.8554	Late-medium season rice
4-84-20120906	93.77	0.9139	Late-medium season rice
457-84-20120915	94.48	0.9122	Late-season rice
457-54-20120915	96.41	0.9387	Late-season rice
455-84-20120916	99.33	0.9875	Late-season rice
2-84-20120919	93.14	0.9027	Late-season rice
2-80-20120919	96.96	0.9494	Late-season rice
7-81-20121001	99.07	0.987	Late-season rice
6-85-20121002	99.8	0.997	Late-season rice
1-88-20121004	99.74	0.9945	Late-season rice
456-88-20121005	99.56	0.9931	Late-season rice

accuracy of 97.04%; for late-season rice identification, the overall kappa coefficient was 0.948 and the overall classification accuracy was 96.46%; for medium-season rice, the overall kappa coefficient was 0.893 and the overall classification accuracy was 92.65%. For classification of the HJ CCD image from July 30, the overall accuracy was only 77.2%, mainly due to cloud contamination. Normally, rice fields of the same season are clustered together for social or environmental reasons, such as location, convenience, or tradition.

5.3 *Results for Mixed-Pixels Identification and Fraction Estimation*

Mixed pixels, which are nearly half of the total, can be effectively identified through image classification. Most mixed pixels are distributed on the fringe of large clusters. After RAFI

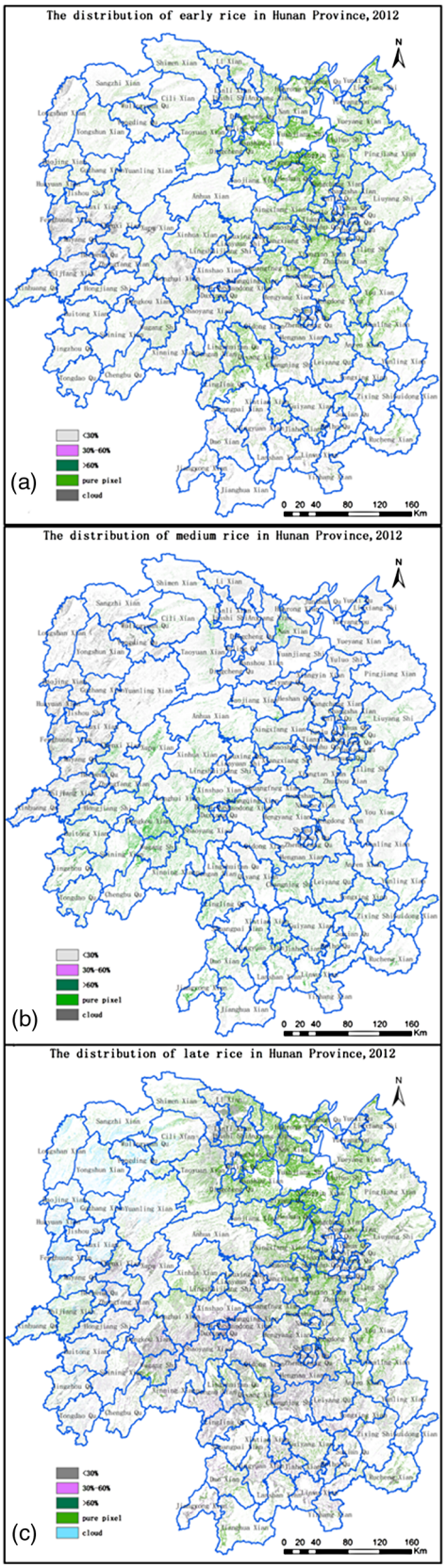

Fig. 8 Rice crop distribution of Hunan Province in 2012. (a) Early-season rice. (b) Medium-season rice. (c) Late-season rice.

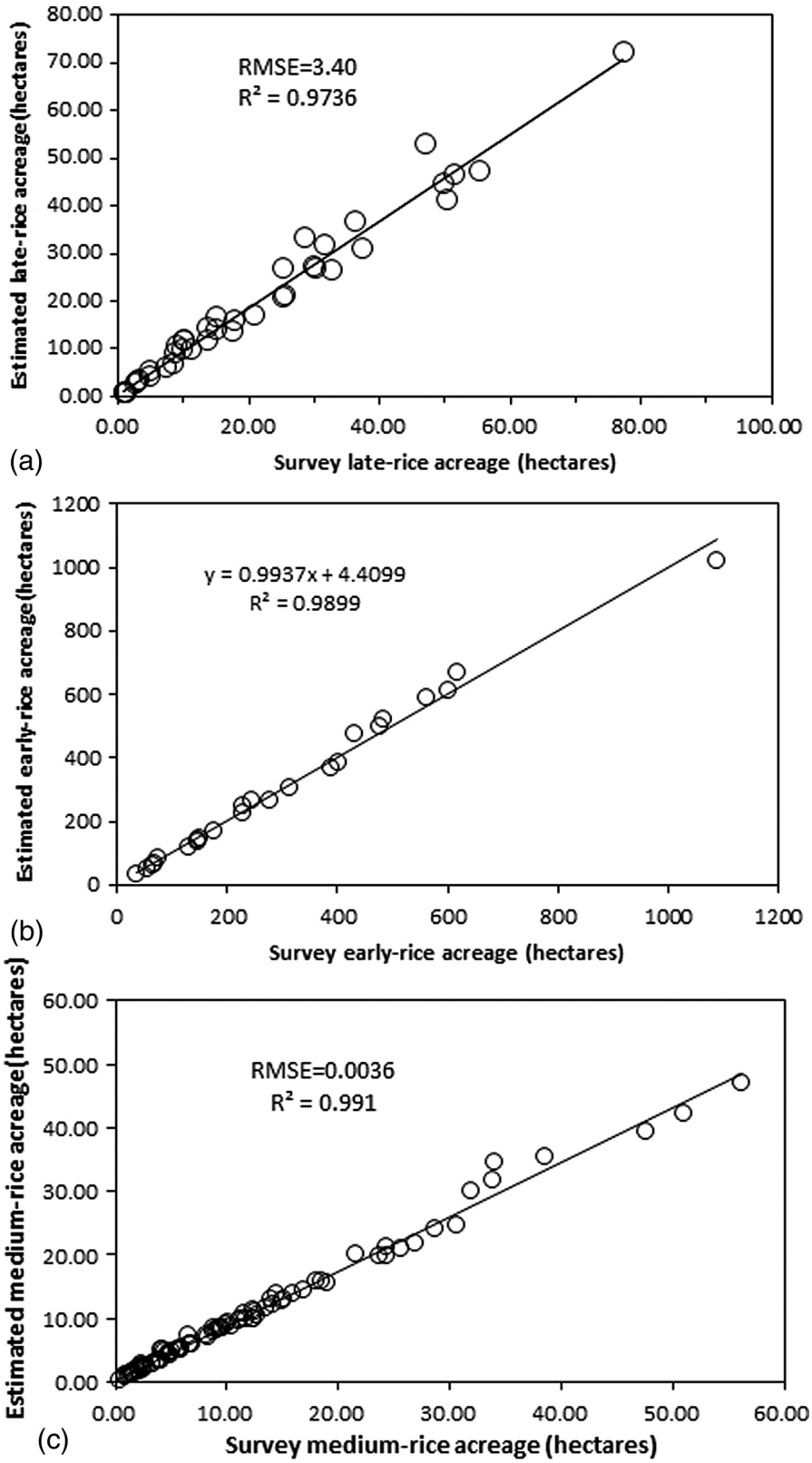

Fig. 9 Validation of rice crop acreage estimation using HJ CCD data. (a) Late-season rice. (b) Early-season rice. (c) Medium-season rice.

calculation for mixed pixels and combination with pure rice crop pixels, all rice crop fields have been identified. Figure 8 shows the final rice crop fraction map combining pure rice crop pixels and the rice crop fraction index using Eqs. (1) and (2).

5.4 *Rice Crop Acreage Estimation Results and Validation*

In 2012, based on the estimation results from this study, 4,307,300 ha of rice were planted in total in Hunan, of which 1,667,200 ha were early-season rice, 1,720,500 ha were late-season rice, and 919,600 ha were medium-season rice. Medium-season rice accounted for ~22.4% of total rice acreage, while early-season and late-season rice accounted for 38.7 and 39.9%, respectively.

Late-season rice acreage was more extensive than that of early-season rice, reflecting rice planting practice in Hunan. Usually, farmers prefer to plant late-season rice even if they did not plant early-season or medium-season rice because of the better quality of late-season rice. Early-season and late-season rice crops were mainly distributed in the eastern part of Hunan Province, e.g., the area surrounding Dongting Lake and the Xiangjiang River Basin, including Yueyang, Changde, Yiyang, Changsha, Xiangtan, Hengyang, Binzhou, and Yongzhou. Medium-season rice was mainly distributed in the southern part of the province, including Xiangxi, Huaihua, Shaoyang, Loudi, and Yongzhou, especially in Shaoyang and Huaihua. Medium-season rice is typically cultivated in the western part where the physical environment is mountainous and hilly. Recently, more and more farmers have turned to planting single-season rice due to labor shortages, in the south.

At the city level, Changde, Yueyang, and Yiyang are listed in the top three areas for double-season rice cropping, accounting for 13.94, 12.38, and 9.86%, respectively, of total rice acreage in Hunan Province. At the county level, Taoyuan, Ningxiang, Hanshou, Dingcheng, and Xiangtan are the top five areas for double-season rice planting, accounting for 3.14, 3.10, 2.94, 2.94, and 2.90%, respectively, of total rice acreage in Hunan Province.

Validation results showed that the acreage estimation results are accurate (Fig. 9) and satisfactory for grain subsidy accounting. For early-season rice, the discrepancy was within 10% at the plot level (6.5×6.5 km). The maximum discrepancy was ~10.65%. The calculated results also show a good relationship between the RapidEye and HJ CCD data ($R^2 = 0.99$). Because the RapidEye data have higher classification accuracy and can reflect ground truth, the early-season rice acreage figures are acceptable. For medium-season and late-season rice, the average discrepancies were 12.20 and 12.36% at the plot level (1×1 km), and the maximum discrepancies were ~19.79 and 20.60%. These results also showed good relationships with *in situ* data at the plot level (1×1 km). The coefficients of determination (R^2) were 0.99 and 0.97, respectively, and the root mean square error (RMSE) values were 0.0036 and 3.40 hectares.

6 Discussion and Conclusions

Recently, the Hunan provincial government has established a series of policies to promote rice cropping, especially double-season rice planting. However, single-season rice cropping practice, which accounted for nearly one third of the total paddy fields in this study, is still expanding.[18] In this study, medium-season rice planting accounted for ~35% of the total rice fields.

For regional rice crop acreage estimation in southern China, wide-swath high-spatial-resolution imagery provided for example by HJ-1 satellites shows an excellent mapping capability; 30% of the area of the province can be covered by two to four cloud-free registrations. Because of serious land fragmentation in eastern China, large numbers of mixed pixels with different crop types are present. In this study, rice crop mixed pixels were present in one third of the total single-season paddy fields. Fuzzy classification is therefore an appropriate tool for subpixel analysis. In this study, subpixel classification using VHR images (<5 m) combined with wide-swath high-resolution data (30-m resolution) was used. Because of the complexity of cropping practice in southern China, remote sensing data with more spectral bands are more suitable for crop discrimination. Short-wave infrared bands can provide soil moisture information to discriminate irrigated crops from other vegetation.[2] Mid-infrared can provide information on lignin and cellulose content, which may also be crucial for crop discrimination. A new

generation of Earth observation satellites, such as Landsat 8 with seven spectral bands, could perform more effectively for identification of different rice crops.

Pixels classified as crops in HJ-1 images contain surfaces including small dykes, roads, large rocks, small huts, and other features. Data from the second National Land Resources Survey for arable land acreage investigation were used to calibrate gross acreage figures to net acreage figures, which were crucial for grain subsidy calculations. NAC could also be used to calculate rice crop acreage even when SAR data were used.

The time-consuming side of the method is mainly the amount of ground sampling required. Hundreds of plots had to be surveyed once or twice every year in addition to the transect survey. For the first one or two years, crop maps from hundreds of plots generated credible spectral training datasets for rice crop identification. After years of operational monitoring, the number of survey plots can be reduced substantially, and a crop spectral profile library containing information on growth stages and corresponding spectral signatures of visible and near-infrared bands can be developed to support spectral training for rice identification. A surer method is to conduct ground surveys in a certain proportion (such as 20%) of croplands and to rotate yearly. In this study, the crop planting intentions of the newest rural households can be collected opportunely in addition to crop mapping in the plots. As for transect surveys using GVG agro-instruments, they provide a good selection of continuous surveys incorporating thousands of geotagged photos to support crop identification using remote sensing data, which compensates for the decrease in the number of plot survey.

Acknowledgments

This study was supported by the Key Research Program of the Chinese Academy of Sciences (Grant No. KZZD-EW-08-05) and the National Natural Science Foundation of China (Grant No. 41071277).

References

1. J. L. Maclean et al., *Rice Almanac: Source Book for the Most Important Economic Activity on Earth*, International Rice Research Institute, CABI Publishing, Philippines (2002).
2. G. D. Badhwar, J. G. Carnes, and W. W. Austin, "Use of landsat-derived temporal profiles for corn-soybean feature extraction and classification," *Remote Sens. Environ.* **12**(1), 57–79 (1982), http://dx.doi.org/10.1016/0034-4257(82)90007-4.
3. S. Fritz et al., "The use of MODIS data to derive acreage estimations for larger fields: a case study in the south-western Rostov region of Russia," *Int. J. Appl. Earth Obs. Geoinf.* **10**(4), 453–466 (2008), http://dx.doi.org/10.1016/j.jag.2007.12.004.
4. B. Wu and Q. Li, "Crop planting and type proportion method for crop acreage estimation of complex agricultural landscapes," *Int. J. Appl. Earth Obs. and Geoinf.* **16**, 101–112 (2012), http://dx.doi.org/10.1016/j.jag.2011.12.006.
5. A. B. Potgieter et al., "Estimating crop area using seasonal time series of enhanced vegetation index from MODIS satellite imagery," *Aust. J. Agric. Res.* **58**(4), 316–325 (2007), http://dx.doi.org/10.1071/AR06279.
6. G. D. Badhwar, C. E. Gargantini, and F. V. Redondo, "Landsat classification of Argentina summer crops," *Remote Sens. Environ.* **21**(1), 111–117 (1987), http://dx.doi.org/10.1016/0034-4257(87)90010-1.
7. D. M. Johnson, "A comparison of coincident Landsat-5 TM and Resourcesat-1 AWiFS imagery for classifying croplands," *Photogramm. Eng. Remote Sens.* **74**(11), 1413–1423 (2008), http://dx.doi.org/10.14358/PERS.74.11.1413.
8. K. Jia et al., "Crop classification using multi-configuration SAR data in the North China Plain," *Int. J. Remote Sens.* **33**(1), 170–183 (2012), http://dx.doi.org/10.1080/01431161.2011.587844.
9. M. E. Jakubauskas, D. R. Legates, and J. H. Kastens, "Crop identification using harmonic analysis of time-series AVHRR NDVI data," *Comput. Electron. Agric.* **37**(1), 127–139 (2002).http://dx.doi.org/10.1016/S0168-1699(02)00116-3

10. Y. Inoue et al., "Normalized difference spectral indices for estimating photosynthetic efficiency and capacity at a canopy scale derived from hyperspectral and CO2 flux measurements in rice," *Remote Sens. Environ.* **112**(1), 156–172 (2008), http://dx.doi.org/10.1016/j.rse.2007.04.011.
11. A. Potgieter et al., "Estimating winter crop area across seasons and regions using time-sequential MODIS imagery," *Int. J. Remote Sens.* **32**(15), 4281–4310 (2011), http://dx.doi.org/10.1080/01431161.2010.486415.
12. B. D. Wardlow and S. L. Egbert, "Large-area crop mapping using time-series MODIS 250 m NDVI data: an assessment for the U.S. Central Great Plains," *Remote Sens. Environ.* **112**(3), 1096–1116 (2008), http://dx.doi.org/10.1016/j.rse.2007.07.019.
13. H. Eerens, *GLIMPSE: Global Image Processing Software User Manual*, Belgium (2004).
14. N. A. Quarmby et al., "Linear mixture modeling applied to AVHRR data for crop area estimation," *Int. J. Remote Sens.* **13**(3), 415–425 (1992), http://dx.doi.org/10.1080/01431169208904046.
15. Q. Z. Li et al., "Maize acreage estimation using ENVISAT MERIS and CBERS-02B CCD data in the North China Plain," *Comput. Electron. Agric.* **78**(2), 208–214 (2011), http://dx.doi.org/10.1016/j.compag.2011.07.008.
16. Y. Shao et al., "Studies on rice backscatter signatures in time domain and its applications," *J. Remote Sens.* **5**(5), 340–345 (2001).
17. W. Koppe et al., "Rice monitoring with multi-temporal and dual-polarimetric TerraSAR-X data," *Int. J. Appl. Earth Obs. Geoinf.* **21**, 568–576 (2013), http://dx.doi.org/10.1016/j.jag.2012.07.016.
18. D. Peng et al., "Detection and estimation of mixed paddy rice cropping patterns with MODIS data," *Int. J. Appl. Earth Obs. Geoinf.* **13**(1), 13–23 (2011), http://dx.doi.org/10.1016/j.jag.2010.06.001.
19. H. Statistic Bureau, *Hunan Statistic Yearbook*, China Statistic Press, Beijing (2010). (in Chinese).
20. K. Jia, B. F. Wu, and Q. Z. Li, "Crop classification using HJ satellite multispectral data in the North China Plain," *J. Appl. Remote Sens.* **7**(1), 073576 (2013), http://dx.doi.org/10.1117/1.JRS.7.073576.
21. E. F. Vermote et al., "Second simulation of the satellite signal in the solar spectrum, 6S: an overview," *IEEE Trans. Geosci. Remote Sens.* **35**(3), 675–686 (1997), http://dx.doi.org/10.1109/36.581987.
22. K. Jia et al., "Accuracy improvement of spectral classification of crop using microwave backscatter data," *Spectrosc. Spectral Anal.* **31**(2), 483–487 (2011).
23. G. M. Foody, "Status of land cover classification accuracy assessment," *Remote Sens. Environ.* **80**(1), 185–201 (2002), http://dx.doi.org/10.1016/S0034-4257(01)00295-4.
24. J. Cohen, "A coefficient of agreement for nominal scales," *Educ. Psychol. Meas.* **20**(1), 37–46 (1960), http://dx.doi.org/10.1177/001316446002000104.
25. J. Sim and C. C. Wright, "The kappa statistic in reliability studies: use, interpretation, and sample size requirements," *Phys. Ther.* **85**(3), 257–268 (2005).
26. J. Chen, J. Huang, and J. Hu, "Mapping rice planting areas in southern China using the China Environment Satellite data," *Math. Comput. Model.* **54**(3), 1037–1043 (2011).

Qiangzi Li is a professor at the State Key Laboratory of Remote Sensing Science, and National Engineering Research Center for Geoinformatics, Institute of Remote Sensing and Digital Earth, Chinese Academy of Sciences. His current research interests include crop acreage and yield estimation using remote sensing.

Huangxue Zhang is a graduate student at the State Key Laboratory of Remote Sensing Science, Jointly Sponsored by the Institute of Remote Sensing and Digital Earth of Chinese Academy of Sciences and Beijing Normal University, China. Her current research interests include agriculture monitoring, crop type identification and crop acreage estimation using remote sensing data.

Xin Du is an assistant professor at the Institute of Remote Sensing and Digital Earth, Chinese Academy of Sciences. His current research interests include crop biomass/yield estimation with remote sensing.

Ning Wen is a deputy director and a senior engineer at the Hunan Planning Institute of Land and Resources (Hunan Research Academy of Geological Sciences). His research includes surveying, mapping and geoinformation.

Qingshan Tao is a surveying engineer at the Hunan Planning Institute of Land and Resources (Hunan Research Academy of Geological Sciences). He is currently engaged in crop acreage and yield estimation using remote sensing, land consolidation and rehabilitation.